Scientia Iranica B (2016) 23(6), 2587–2594

Sharif University of Technology
Scientia Iranica
Transactions B: Mechanical Engineering
www.scientiairanica.com

Mixed-convection boundary-layer flow of Sisko fluid along a stretching cylinder in a thermally stratified medium

M.Y. Malik, M. Awais*, **T. Salahuddin, A. Hussain and S. Bilal**

Department of Mathematics, Quaid-i-Azam University, Islamabad 44000, Pakistan.

Received 19 October 2014; received in revised form 11 October 2015; accepted 30 January 2016

KEYWORDS
Sisko fluid model;
Mixed convection;
Boundary-layer flow;
Thermally stratified medium;
Stretching cylinder;
Shooting method.

Abstract. The aim of this paper is to figure out the flow and heat problem of two-dimensional steady axisymmetric laminar mixed-convection boundary-layer flow of Sisko fluid model along a stretching cylinder in a thermally stratified medium. The similarity transformations are used to reduce coupled partial differential equations to ordinary differential equations. To solve these equations, a numerical approach called shooting method has been used for the computation of different physical parameters of velocity and temperature field, respectively. The dependence of skin friction and Nusselt number has been analyzed in details in tables.

1. Introduction

During the last two decades, flow of non-Newtonian fluids has been involved in various physical phenomena, such as polymer processing, ink-jet printing, geological flows on the earth mantle, liquid crystals, additive suspensions, animal blood, turbulent shear flows, and many others. In the available literature regarding flow of non-Newtonian fluids and its extensive use in industrial and technological applications, special attention has been paid to these fluids. Therefore, several fundamental equations have been suggested to predict the physical behavior and structure of such fluids. Among these, a comparatively simple model, named Sisko fluids, exists. The Sisko fluid model is the combination of Newtonian and non-Newtonian fluids. The fluid model is capable of describing shear thinning and shear thickening phenomena, which represent decrease and increase in viscosity with increasing shear rate, respectively. This type of fluids exist commonly in nature. Such fluids are well known and have many industrial applications. For the flow of greases, it is the most relevant model. Sisko [1] was the first person who presented and analyzed the lubricating grease. Afterwards, many researchers worked on this model. Munir et al. [2] characterized the effect of steady flow of Sisko fluid with buoyancy assisting and opposing mixed convection over an isothermal stretching surface. They perceived that with an increase in material parameter of Sisko fluid, skin friction increased. Munir et al. [3] also performed the heat transfer analysis of mixed convection Sisko fluid with viscous dissipation rates. Khan et al. [4,5], Nadeem et al. [6], Akbar [7], Ellahi et al. [8-11] and many others investigated the non-Newtonian fluid model in different geometries with pertinent physical properties of fluid.

Convection is the transfer of heat from one place to another place due to transfer of molecules, which plays an important role in practical models. The convective heat transfer mode includes two mechanisms. In addition to energy transfer due to random molecular motion (diffusion), energy is also transferred

*. *Corresponding author. Tel.: +92 33 45144858*
E-mail addresses: drmymalik@hotmail.com (M.Y. Malik); awais88.math@gmail.com (M. Awais); taimoor_salahuddin@yahoo.com (T. Salahuddin); alihassan721214@gmail.com (A. Hussain); sardarbilal111@yahoo.com (S. Bilal)

by the bulk or macroscopic motion of the fluid. The contribution due to bulk fluid motion occurs in the boundary layer. Convection may be natural, free, or mixed. The convection which involves the combined effects of natural and forced convections is known as mixed convection. Many convection processes take place in our surroundings, such as electric devices cooled by fans, nuclear reactors cooled during emergency shutdown, heat exchanges occurring in a low-velocity environment, flows in the ocean and in the atmosphere, etc. Fluid movement during convection may be invisibly slow, or it may be obvious and rapid as in a hurricane. Due to its abundant use in nature, mixed convection has been studied by many scientists. Sheikholeslami et al. [11] performed heat transfer analysis of natural convective nanofluid enclosure with elliptic inner cylinder. Bachok and Ishak [12] analyzed mixed-convection boundary-layer flow over a permeable vertical cylinder with prescribed surface heat flux. Heckel et al. [13] also examined mixed convection along slender vertical cylinders with variable surface temperature. Hsiao [14] explored MHD mixed convection for viscoelastic fluid passing a porous wedge. Chen [15] discussed laminar mixed convection adjacent to vertical, continuously stretching sheet. Nadeem and Saleem [16] analyzed unsteady mixed-convection flow of nanofluid on a rotating cone with magnetic field. Buchlin [17] inspected natural and forced convective heat transfers on slender cylinders.

Stratification effects in any fluid may happen due to temperature variation or concentration differences or the presence of different fluids in any medium or combination of them. As fluid heats and cools, it expands and contracts, causing change in density. This is called thermal stratification and generally occurs when thermal energy transforms from heated bodies and thermal sources into the medium. Stratification may also arise due to concentration differences such as transport processes in the sea where stratification exists due to salinity variation. Third type of stratification occurs when fluids having different densities are present and stable situation arises such that the fluid having less density overlies the heavier fluid. Stratification may double in practical situations, where the heat and mass transfer mechanisms run parallel. Stratification has abundant application in our real world. Applications of stratification include heat extraction into the environment such as from lakes, rivers, and seas. Thermal energy storage systems such as solar ponds and heat transfer from thermal sources such as the condensers of power plants are also examples of stratification. Due to numerous implementations in fluid mechanics, many researchers have worked on stratification phenomenon. The flow due to a heated surface immersed in a stable stratified medium has been investigated experimentally and analytically in several studies such as Yang et al. [18], Jaluria and Gebhart [19], Chen and Eichhorn [20], Ishak et al. [21], Mukhopadhyay et al. [22], and Mansour [23] etc.

The main objective of this paper is to examine the behavior of mixed-convection boundary-layer flow of Sisko fluid over the stretching cylinder in a stratified medium, which has not been discussed so far. The final nonlinear differential equations are solved numerically by shooting method. The influence of curvature parameter, M, material parameter, A, mixed convection parameter, λ, stratification parameter, S, and Prandtl number, Pr, on velocity and temperature profile is discussed.

2. Mathematical formulation

Let us consider the two-dimensional steady axisymmetric flow of an incompressible mixed-convection boundary-layer flow of Sisko fluid over a stretching cylinder. Under these suppositions, along with the boundary layer approximations, the conducted equations which model the problem under consideration are:

$$\frac{\partial(ru)}{\partial x}+\frac{\partial(rv)}{\partial r}=0, \tag{1}$$

$$u\frac{\partial u}{\partial x}+v\frac{\partial u}{\partial r}=\frac{a}{r\rho}\frac{\partial}{\partial r}\left(r\frac{\partial u}{\partial r}\right)+\frac{b}{r\rho}\left(-\frac{\partial u}{\partial r}\right)^{n}-\frac{nb}{r\rho}\left(-\frac{\partial u}{\partial r}\right)^{n-1}\frac{\partial^2 u}{\partial r^2}+g\beta(T_p-T_\infty), \tag{2}$$

$$u\frac{\partial T}{\partial x}+v\frac{\partial T}{\partial y}=\frac{k}{r}\frac{\partial}{\partial r}\left(r\frac{\partial T}{\partial r}\right), \tag{3}$$

subjected to the boundary conditions:

$$u=U(x), \qquad v=0, \qquad T=T_w(x) \quad \text{at} \quad r=r_0,$$

$$u\to 0, \qquad T\to T_\infty(x) \quad \text{as} \quad r\to\infty. \tag{4}$$

In the above expressions, u and v are the velocity components in the x and r directions, respectively, ρ is fluid density, k is thermal diffusivity of the fluid, n is the power law index, $T_w(x)=T_0+b(x/L)$ is the prescribed surface temperature, $T_\infty(x)=T_0+c(x/L)$ is the variable ambient temperature, r_0 is the radius of the cylinder, and a and b are the material constants. It is assumed that the convecting fluid and the medium are in local thermodynamic equilibrium. Stream function ψ is defined as:

$$u=\frac{1}{r}\frac{\partial\psi}{\partial r}, \qquad v=\frac{-1}{r}\frac{\partial\psi}{\partial x}. \tag{5}$$

To get similarity solutions of Eqs. (1)-(3) subject to the boundary conditions in Eq. (4), we introduce the following similarity transformation:

$$\eta = \frac{r^2 - r_0^2}{2r_0 x}\mathrm{Re}_b^{\frac{1}{n+1}}, \qquad \psi = r_0 x U \mathrm{Re}_b^{-\frac{1}{n+1}} f(\eta),$$

$$\theta(\eta) = \frac{T - T_\infty}{T_w - T_\infty}, \qquad \mathrm{Re}_b = \frac{\rho U^{2-n} x^n}{b}, \quad U = cx. \quad (6)$$

Eq. (5) identically satisfies the continuity equation (Eq. (1)). Substituting Eq. (5) into Eqs. (2) and (3) gives:

$$A(1+2M\eta)f''' + n(1+2M\eta)^{\frac{n+1}{2}}(-f'')^{n-1}f'''$$
$$+ 2MAf'' - (n+1)M(1+2M\eta)^{\frac{n-1}{2}}(-f'')^n$$
$$+ \frac{2n}{n+1}ff'' - f'^2 + \lambda\theta = 0, \quad (7)$$

$$(1+2M\eta)\theta'' + 2M\theta' + \mathrm{Pr}\left(\frac{2n}{n+1}\theta' f - f'\theta - Sf\right) = 0, \quad (8)$$

$$f(0) = 0, \quad f'(0) = 1, \quad \theta(0) = 1 - S \quad \text{at} \quad \eta = 0,$$
$$f'(\infty) \to 0, \quad \theta(\infty) \to 0. \quad \text{at} \quad \eta \to \infty, \quad (9)$$

where dimensionless quantities, i.e. Prandlt's number, Pr, material parameter, A, mixed-convection parameter, λ, and curvature parameter, M, are defined as:

$$\mathrm{Pr} = \frac{xU}{k\mathrm{Re}_b^{\frac{2}{n+1}}}, \qquad A = \frac{\mathrm{Re}_b^{\frac{2}{n+1}}}{\mathrm{Re}_a},$$

$$\lambda = \frac{gBx(T_p - T_\infty)}{U^2}, \qquad M = \frac{x}{r_0 \mathrm{Re}_b^{\frac{1}{n+1}}},$$

$$\mathrm{Re}_a = \frac{\rho U x}{a}, \qquad \mathrm{Re}_b = \frac{\rho U^{2-n} x^n}{b}. \quad (10)$$

Skin friction and local Nusselt number can be defined as:

$$C_f = \frac{\tau_w}{\rho c (cv)^{\frac{1}{2}}}, \qquad \mathrm{Nu}_x = \frac{x q_w}{k(T_p - T_\infty)}, \quad (11)$$

$$\tau_w = a\left(\frac{\partial u}{\partial r}\right)_{r=r_0} - b\left(-\frac{\partial u}{\partial r}\right)^n_{r=r_0},$$

$$q_w = -k\left(\frac{\partial T}{\partial r}\right)_{r=r_0}, \quad (12)$$

while the dimensionless forms of skin friction and local Nusselt number are:

$$\frac{1}{2}C_f \mathrm{Re}_b^{\frac{1}{n+1}} = Af''(0) - (-f'''(0))^n,$$

$$\mathrm{Nu}_x \mathrm{Re}_b^{\frac{1}{n+1}} = -\theta'(0). \quad (13)$$

3. Numerical solutions

As we know that the non-linear momentum, Eq. (7), is the third order in f and non-linear energy, Eq. (8), is the second order in θ, total order of both equations is 5, which can be diminished to a system of five first-order ordinary differential equations with five unknowns. In order to solve these equations, we use a numerical technique, "Runge-Kutta Fehlberg" method. To solve our system of equations, we must have five initial conditions; but, as we know, we have only two initial conditions in f and one initial condition in θ that have been known, i.e. one initial condition of f and one of θ are missing. However, the values of f and θ are known at $\eta \to \infty$. Thus, these two end conditions are exploited to produce two unknown initial conditions. The most important step of this method is to choose the appropriate finite value of η_∞. Thus, to estimate the value of η_∞, we start with some initial guess and solve the boundary value problem consisting of Eqs. (7) and (8) to obtain $f''(0)$ and $\theta'(0)$. The solution process is repeated with another larger value of η_∞ until two successive values of $f''(0)$ and $\theta'(0)$ differ only after the desired significant digit. The last value of η_∞ is taken as the finite value of the limit η_∞ for the particular set of physical parameters for determining velocity $f(\eta)$ and $\theta(\eta)$ in the boundary layer. After getting all the five initial conditions, we solve this system of simultaneous equations using order Runge-Kutta Fehlberg integration scheme.

4. Discussion

Now, we have to explore the graphical behavior of different specifications of velocity and temperature fields. Figures 1 and 2 describe the behavior of velocity profile for different values of A for $n = 1$ and 2. It is

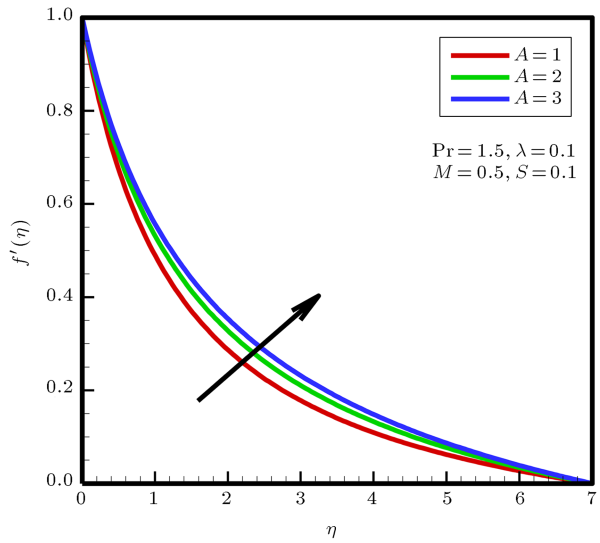

Figure 1. Effect of A on $f'(\eta)$ for $n = 1$.

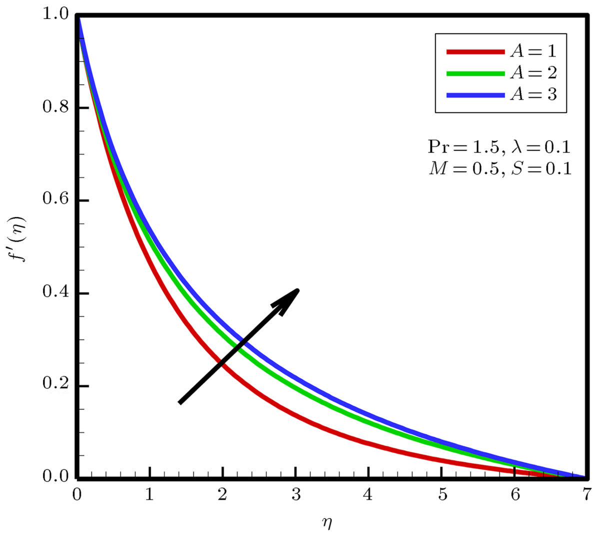

Figure 2. Effect of A on $f'(\eta)$ for $n = 2$.

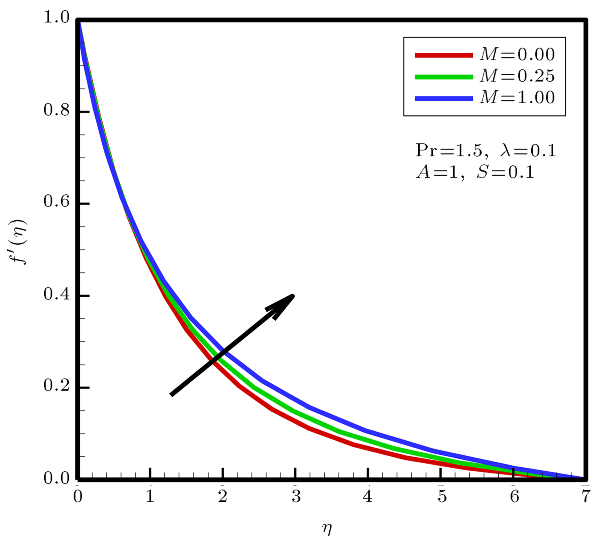

Figure 3. Effect of M on $f'(\eta)$ for $n = 1$.

observed that velocity increases as A increases. The effect of increasing values of the material parameter A is to enhance the velocity field and hence the boundary layer thickness.

Now, we concentrate on the influence of the curvature parameter, M, on the velocity profile, which is shown in Figures 3 and 4. It is examined that with the increase of curvature parameter, M, velocity field increases. The reason is that by increasing curvature parameter, M, radius of curvature decreases, which implies that area of the cylinder decreases with the fluid. Thus, area of connectivity of fluid and cylinder is decreases as less resistance is offered by surface of the cylinder; therefore, velocity of the fluid increases.

Figures 5 and 6 demonstrate the behavior of the mixed-convection parameter λ for $n = 1$ & 2 on velocity field. It is perceived that velocity of the fluid increases with an increase in the mixed-convection parameter, λ.

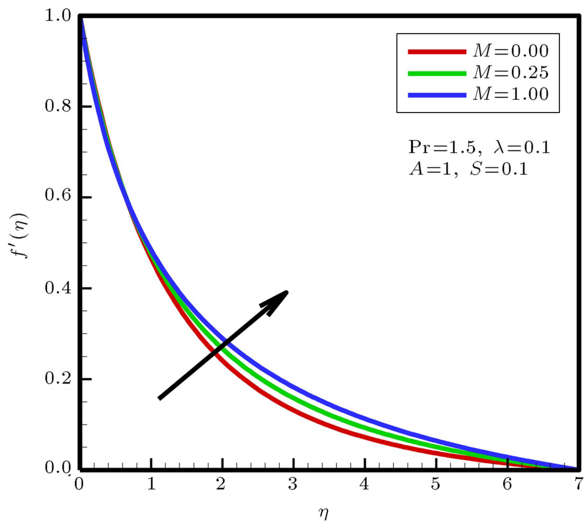

Figure 4. Effect of M on $f'(\eta)$ for $n = 2$.

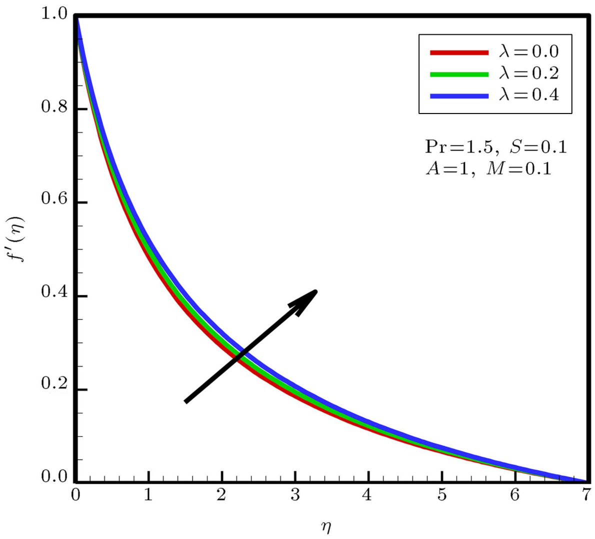

Figure 5. Effect of λ on $f'(\eta)$ for $n = 1$.

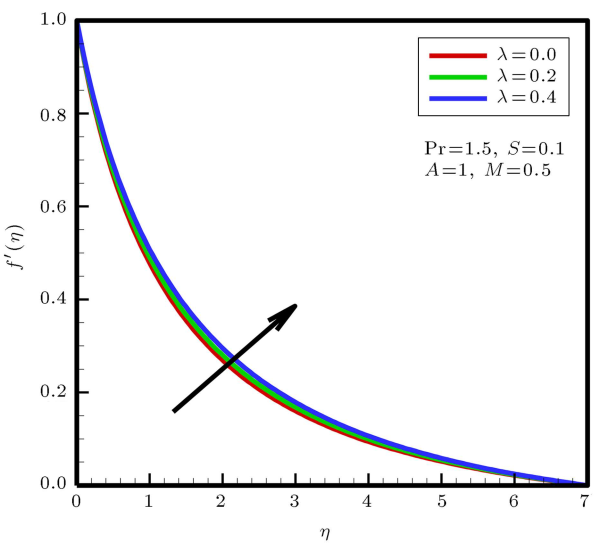

Figure 6. Effect of λ on $f'(\eta)$ for $n = 2$.

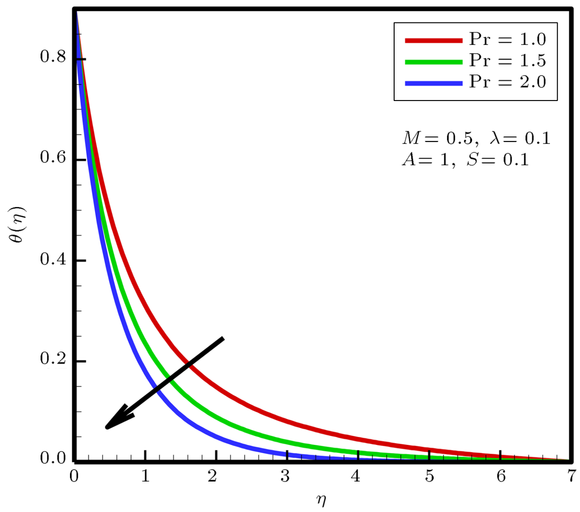

Figure 7. Effect of Pr on $\theta(\eta)$ for $n = 1$.

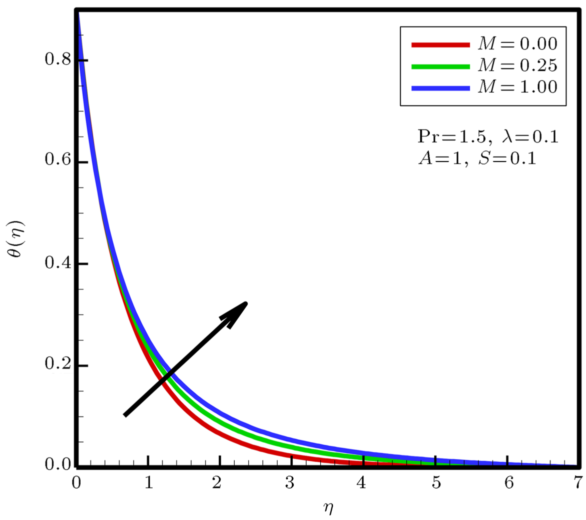

Figure 9. Effect of M on $\theta(\eta)$ for $n = 1$.

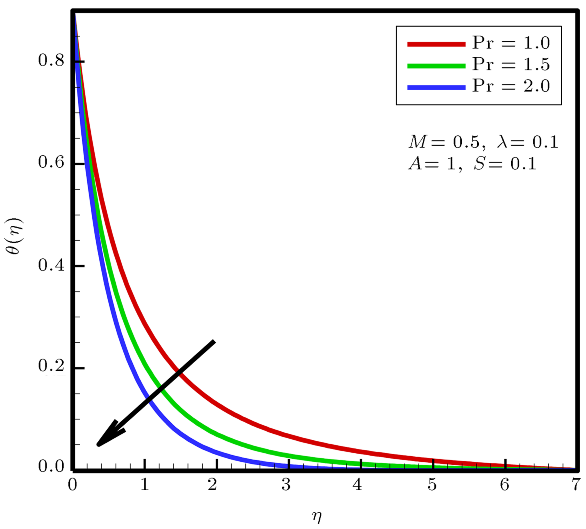

Figure 8. Effect of Pr on $\theta(\eta)$ for $n = 2$.

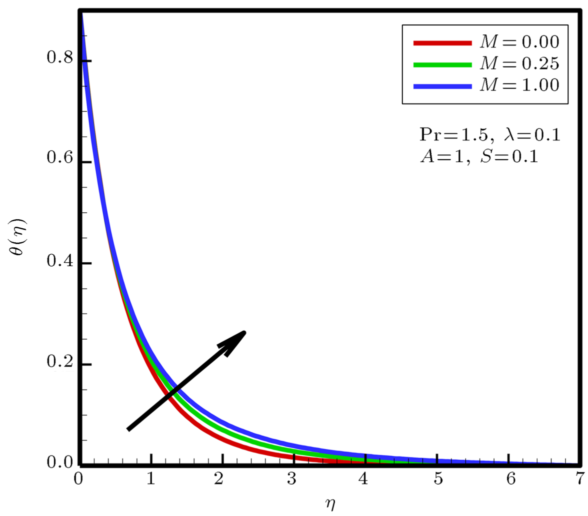

Figure 10. Effect of M on $\theta(\eta)$ for $n = 2$.

Because λ is the ratio of buoyancy to inertial forces, by increasing mixed-convection parameter, λ, buoyancy forces increase as a result of velocity increase.

Figures 7 and 8 are plotted for different values of Prandtl number for $n = 1$ & 2 on temperature field. It is depicted that temperature field decreases. For larger values of Prandtl number, thermal boundary-layer thickness reduces. The Prandtl number signifies the ratio of momentum diffusivity to thermal diffusivity. Hence, for large value of Prandtl number, Pr, the thermal conductivity decreases and this causes decrease in temperature.

The attribute of curvature M for $n = 1$ & 2 on temperature field is shown in Figures 9 and 10. It is observed that temperature increases with an increase in curvature parameter; also, as surface area decreases due to this, the transfer of energy increases.

The effects of the stratification parameter S on the temperature and its gradient for $n = 1$ and 2 are revealed in Figures 11-14. Since stratification decreases temperature in the boundary layer, temperature gradient decreases. Also, when stratification parameter, S, increases, thickness of thermal boundary layer reduces. Difference between surface and ambient temperature decreases in the boundary layer for higher values of S. Ambient thermal stratification causes a significant decrease in the local buoyancy levels, which reduces the velocities in the boundary layer. All temperature profiles decay from the maximum value at the wall to zero in the free stream, that is, converge at the outer edge of the boundary layer. Table 1 presents the values of Skin-friction coefficient for different values of physical parameters. It is noted that the Skin-friction coefficient increases with increasing the physical parameters A and M and decreases with increase in λ.

Table 2 displays the result of local Nusselt number for different values of parameters M and Pr. It can be seen form Tables 1 and 2 that as we increase the values

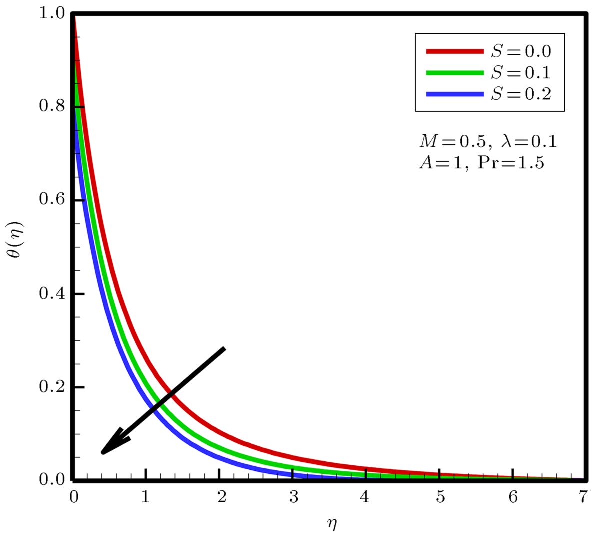

Figure 11. Effect of S on $\theta(\eta)$ for $n = 1$.

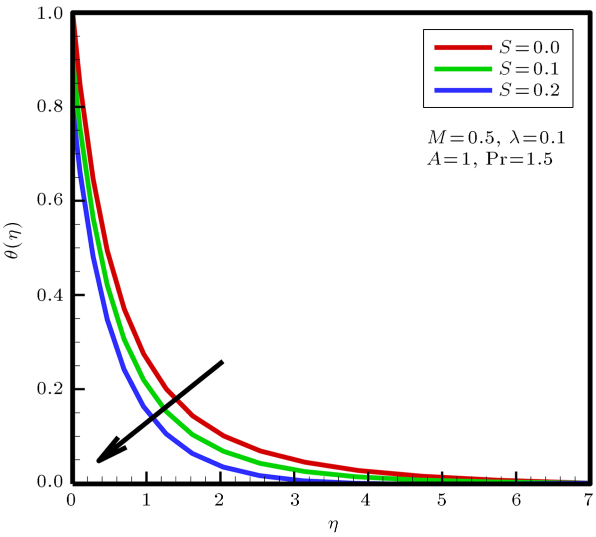

Figure 12. Effect of S on $\theta(\eta)$ for $n = 2$.

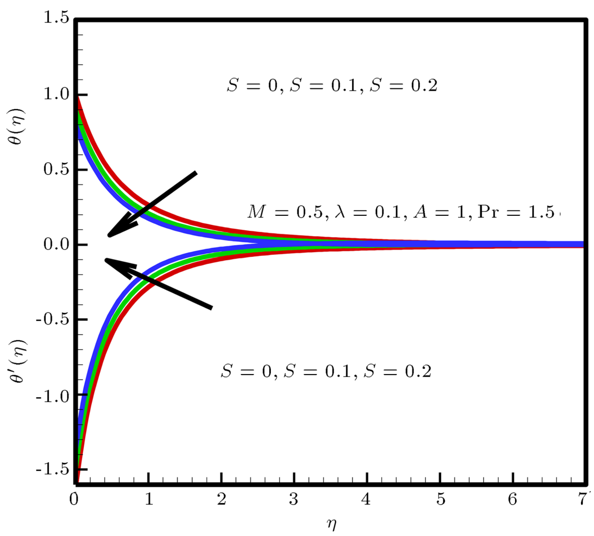

Figure 13. Effect of S on $\theta(\eta)$ and $\theta'(\eta)$ for $n = 1$.

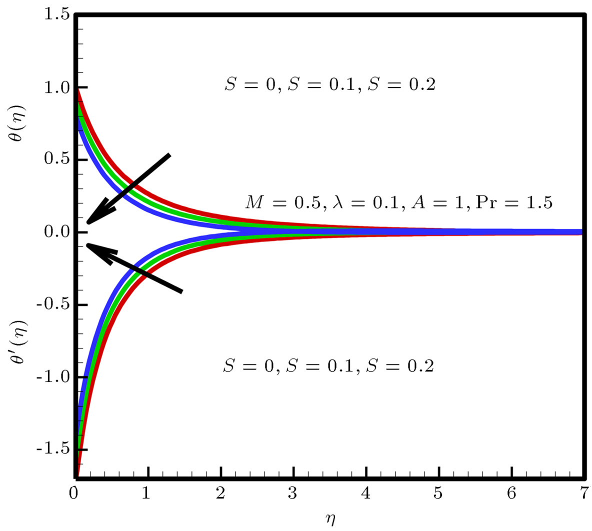

Figure 14. Effect of S on $\theta(\eta)$ and $\theta'(\eta)$ for $n = 2$.

Table 1. The variation of skin-friction coefficient with respect to M, A, and λ for $n = 1$ and 2.

M	A	λ	$n = 1$ $(1+A)f''(0)$	$n = 2$ $Af''(0)-(f''(0))^2$
0	1	0.1	-1.6793	-1.3896
0.5	–	–	-1.8424	-1.7097
1	–	–	-2.1342	-1.9451
0.5	1	–	-1.8424	-1.7097
–	2	–	-2.4577	-2.1595
–	3	–	-3.0506	-2.7143
–	1	0.1	-1.8424	-1.7097
–	–	0.2	-1.8036	-1.6696
–	–	0.3	-1.7651	-1.6213

Table 2. The variation of $-\theta'(0)$ with respect to Pr, M and, S for $n = 1$ and 2.

Pr	M	S	$n = 1$ $-\theta'(\eta)$	$n = 2$ $-\theta'(0)$
1	0.5	0.1	1.2136	1.2832
2	–	–	1.7179	1.8203
3	–	–	2.1168	2.2406
1.5	0	–	1.4113	1.4349
–	0.5	–	1.4832	1.5047
–	1	–	1.6314	1.6542
–	0.5	0	1.5444	1.5234
	–	0.1	1.4832	1.4799
	–	0.2	1.4319	1.4147

of curvature parameter M and Prandtl number Pr, the value of Nusselt number increases.

5. Concluding remarks

The main findings of the present analysis are listed below:

- The behavior of curvature parameter M for different velocity and temperature fields is the same, i.e. both velocity and temperature fields increase with velocity and temperature;
- Velocity increases with an increase in material parameter A;
- By increase in mixed convection parameter, λ, velocity increases;
- With an increase in Prandtl number, Pr, temperature decreases;
- The Stratification parameter S decreases as temperature profile decreases.

References

1. Sisko, A.W. "The flow of lubricating greases", *Ind. Eng. Chem. Res.*, **50**, pp. 1789-1792 (1958).
2. Munir, A., Shahzad, A. and Khan, M. "Mixed convection heat transfer in Sisko fluid with viscous dissipation: Effects of assisting and opposing buoyancy", *Chemical Engineering Research and Design*, **97**, pp. 120-127 (2015).
3. Munir, A., Shahzad, A. and Khan, M. "Convective flow of Sisko fluid over a wedge with viscous dissipation", *Journal of the Brazilian Society of Mechanical Sciences and Engineering*, pp. 1-7 (2015).
4. Khan,. M. and Abbas, Z. "Analytic solution for flow of Sisko fluid through a porous medium", *Transp. Porous. Med.*, **71**, pp. 23-37 (2008).
5. Khan, M., Munawar, S. and Abbasbandy, S. "Steady flow and heat transfer of a Sisko fluid in annular pipe", *Int. J. Heat. Mass. Transf.*, **53**, pp. 1290-1297 (2010).
6. Nadeem. S. and Akbar, N.S. "Peristaltic flow of Sisko fluid in a uniform inclined tube", *Acta. Mech. Sin.*, **26**, pp. 675-683 (2010).
7. Akbar, N.S. "Peristaltic Sisko nano fluid in an asymmetric channel, App", *Nano Sci.*, **4**, pp. 663-673 (2014).
8. Ellahi, R. "The thermodynamics, stability, applications and techniques of differential type: a review", *Reviews in Theoretical Science*, **2**, pp. 116-123 (2014).
9. Ellahi, R. "The effects of MHD and temperature dependent viscosity on the flow of non-Newtonian nanofluid in a pipe: analytical solutions", *Applied Mathematical Modeling*, **37**(3), pp. 1451-1457 (2013).
10. Zeeshan, A. and Ellahi, R. "Series solutions of nonlinear partial differential equations with slip boundary conditions for non-Newtonian MHD fluid in porous space", *Journal of Applied Mathematics & Information Sciences*, **7**(1), pp. 253-261 (2013).
11. Sheikholeslami, M., Ellahi, R., Hassan, M. and Soleimani, S. "A study of natural convection heat transfer in a nanofluid filled enclosure with elliptic inner cylinder", *International Journal for Numerical Methods for Heat and Fluid Flow*, **24**(8), pp. 1906-1927 (2014).
12. Bachok, N. and Ishak, A. "Mixed convection boundary layer flow over a permeable vertical cylinder with prescribed surface heat flux", *European J. Scientific Research*, **34**, pp. 46-54 (2009).
13. Heckel, J.J., Chen, T.S. and Armaly, B.F. "Mixed convection along slender vertical cylinders with variable surface temperature", *Int. J. Heat. Mass. Transf.*, **32**, pp. 431-1442 (1989).
14. Hsiao, K.L. "MHD mixed convection for viscoelastic fluid past a porous wedge", *Int J. Non-Linear Mech.*, **46**, pp. 1-8 (2011).
15. Chen, C.H. "Laminar mixed convection adjacent to vertical, continuously stretching sheet", *Int. J. Heat. Mass. Transf.*, **33**, pp. 471-476 (1998).
16. Nadeem, S. and Saleem, S. "Unsteady mixed convection flow of nanofluid on a rotating cone with magnetic field", *App. Nano. Sci.*, **4**, pp. 405-414 (2014).
17. Buchlin, J.M. "Natural and forced convective heat transfer on slender cylinders", *Revue Generale de Thermique*, **33**, pp. 653-660 (1998).
18. Yang, K.T., Novotny, J.L. and Cheng, Y.S. "Laminar free convection from a non-isothermal plate immersed in a temperature stratified medium", *Int. J. Heat. Mass. Transf.*, **15**, pp. 1097-1109 (1972).
19. Jaluria, Y. and Gebhart, B. "Stability and transition of buoyancy-induced flows in a stratified medium", *J. Fluid Mech.*, **66**, pp. 593-612 (1974).
20. Chen, C.C., and Eichhorn, R. "Natural convection from simple bodies immersed in thermally stratified fluids", *The ASME J. Heat Transf.*, **98**, pp. 446-451 (1976).
21. Ishak, A., Nazar, R. and Pop, I. "Mixed convection boundary layer flow adjacent to a vertical surface embedded in a stable stratified medium", *Int. J. Heat. Mass. Transf.*, **51**, pp. 3693-3695 (2008).
22. Mukhopadhyay, S., Mondal, I.C. and Gorla, R.S. "Effects of thermal stratification on flow and heat transfer past a porous vertical stretching surface", *Heat Mass Transf.*, **48**, pp. 915-921 (2012).
23. Mansour, M.A., Mohamed, R.A., Abd-Elaziz, M.M. and Sameh, E.A. "Thermal stratification and suction/injection effects on flow and heat transfer of micropolar fluid due to stretching cylinder", *Int. J. Numer. Meth. Biomed. Engng.*, **27**, pp. 1951-1963 (2011).

Biographies

Muhammad Yousaf Malik is a Professor of Mathematics at Quaid-i-Azam University, Islamabad, Pakistan. He received his M.Phil. degree from Quaid-i-Azam University, Islamabad, in 1988, and PhD from

University of Bradford, UK, in 2000 and specialization in computational fluid dynamics. He has many published research articles in the field of fluid dynamics, computational fluid dynamics, heat transfer and extended surfaces in well-known International Journals.

Muhammad Awais is a PhD Candidate in Department of Mathematics at Quaid-i-Azam University, Islamabad, Pakistan, under the supervision of Dr. Muhammad Yousaf Malik. He has obtained his M.Phil. degree with distinction in 2015 from Quaid-i-Azam University, Islamabad, Pakistan, in applied mathematics. He has many published research articles in the field of fluid dynamics, computational fluid dynamics and heat transfer in well-known International Journals.

Taimoor Salahuddin is a PhD Candidate in Department of Mathematics at Quaid-i-Azam University, Islamabad, Pakistan, under the supervision of Dr. Muhammad Yousaf Malik. He has received his M.Phil. degree from Quaid-i-Azam University, Islamabad, Pakistan, in 2012. He has many published research articles in the field of fluid dynamics, computational fluid dynamics, and heat transfer in well-known International Journals.

Arif Hussain is a PhD Candidate in Department of Mathematics at Quaid-i-Azam University, Islamabad, Pakistan, under the supervision of Dr. Muhammad Yousaf Malik. He has done his M.Phil. degree from Quaid-i-Azam University, Islamabad, Pakistan in 2015. He has many published research articles in the field of fluid dynamics in well-known International Journals.

Sardar Bilal is a PhD Candidate in Department of Mathematics at Quaid-i-Azam University, Islamabad, Pakistan, under the supervision of Dr. Muhammad Yousaf Malik. He has received his M.Phil. degree from Quaid-i-Azam University, Islamabad, Pakistan, in 2013. He has many published research articles in the field of fluid dynamics in well-known International Journals.